

**Effective interaction in two-dimensional electron systems**

Takeshi Suwa and Kazuo Takayanagi

*Department of Physics, Sophia University, Kioi-cho, Chiyoda-ku, Tokyo 102-8554, Japan*

Enrico Lipparini

*Department of Physics, University of Trento, Povo(Trento) 38050, Italy*

(Received 27 December 2002; revised manuscript received 10 November 2003; published 10 March 2004)

A fully microscopic derivation is proposed for an effective interaction operator between electrons in the two-dimensional electron gas (2DEG), which represents multiple-scattering processes in the medium. The obtained interaction features short-range behaviors between electrons, and is presented in a simple form which allows applications in various systems. Short-range correlation in the 2DEG is discussed in detail in terms of the effective interaction with special emphasis on the nonlocal aspect of the correlation.

DOI: 10.1103/PhysRevB.69.115105

PACS number(s): 71.10.Ca, 21.30.Fe, 73.21.Fg

**I. INTRODUCTION**

Recent developments of experimental devices<sup>1</sup> allowed one to obtain plenty of information on static as well as dynamic properties of various finite and bulk two-dimensional electron systems. At the same time much effort has been devoted to theoretical investigations of these systems.

Ground-state properties of the bulk systems, especially the correlation energies, have been studied for a long time by a variety of many-body theories, including random-phase approximation (RPA),<sup>2</sup> perturbation theory,<sup>3</sup> local-field theory,<sup>4</sup> coupled-cluster theory,<sup>5</sup> quantum kinetic theory,<sup>6</sup> and ladder approximation.<sup>7</sup> The importance of the short-range correlation has been repeatedly emphasized in these different theoretical schemes, which is now realized also in the study of experimentally accessible phenomena.<sup>8</sup> In this situation we believe that it is important to investigate the short-range correlation directly by realizing it as an effective interaction operator.

In this paper we construct an effective electron-electron interaction which takes into account the effect of the short-range correlations. On one hand, our work is based on the analysis of the multiple-scattering processes in the medium, and is similar in concept to that of Nagano, Singwi, and Ohnishi,<sup>7</sup> which calculated the correlation energy by summing up all the ladder processes. On the other hand, our method is closely related to the derivation of an effective interaction operator, which is a well-known concept in the field of nuclear physics,<sup>9-12</sup> and has been applied to three-dimensional (3D) electron systems.<sup>13,14</sup>

It is well known that the ladder processes are expressed as the  $G$  operator defined by the Bethe-Goldstone equation. It is, however, a very long way to express the  $G$  operator as a tractable two-body interaction operator, which is conventionally given by a certain prescription which has only a vague physical basis with no way of checking its validity.<sup>15</sup>

In this work, we propose a fully microscopic derivation of an effective interaction operator from the Bethe-Goldstone equation with the newly introduced exact Pauli operator, and examine the short-range correlation directly.

The plan of the work is the following. In Sec. II we explain in detail the derivation of the momentum-dependent

zero-range effective interaction of Skyrme-type.<sup>16</sup> The calculated interaction is shown to be applicable to the description of the ground and low-lying excited states. In Sec. III we give numerical results and discussions. All the parameters of the effective interaction are given explicitly as functions of the Wigner-Seitz parameter  $r_s$ . The properties of the effective interaction are discussed in detail in connection with the local and nonlocal features of the correlation effects and also with the competition between the  $s$ - and  $p$ -wave correlations. We also estimate the importance of the three-body correlation compared to the two-body correlation. Finally, the short-range correlation is discussed in terms of the pair-correlation function  $g(r)$  and the correlation energy. We also compare the exact and the angle-averaged Pauli operators using these physical quantities. In Sec. IV we give a brief summary.

**II. EFFECTIVE ELECTRON-ELECTRON INTERACTION**

The concept of the effective interaction has been widely used in nuclear physics, because it significantly simplifies the description of many-body systems by transferring a part of the complexities from the wave function to the Hamiltonian. In this section we derive an effective interaction which represents the short range correlation in the two-dimensional electron gas (2DEG) with a neutralizing positive background. We adopt the atomic units where  $\hbar = m_e = e$  (minus of electron charge) = 1. The density  $\rho$  of the system is specified by the Wigner-Seitz parameter  $r_s$  by  $1/\rho = \pi r_s^2$ . Our system has no spin polarization, and the Fermi momentum is given by  $k_f = \sqrt{2}/r_s$ . In the following we suppress the spin indices for simplicity.

**A.  $g$  matrix**

In order to construct a two-body effective interaction, we concentrate on the two-body correlations between electrons that are represented by multiple-scattering processes in the medium. These processes are described by the  $G$  operator which is the solution to the Bethe-Goldstone equation,<sup>9-13</sup>

$$G = V + V \frac{Q}{\omega - H_0} G, \quad (1)$$

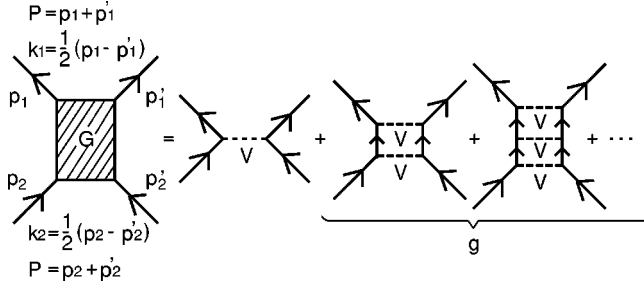


FIG. 1. Graphical representation of Eqs. (1) and (2). The dashed lines represent the bare Coulomb interaction  $V$ , and  $g$  is the correction due to the multiple-scattering processes. The relative momenta for the final and the initial states are given by  $\mathbf{k}_1 = (\mathbf{p}_1 - \mathbf{p}'_1)/2$  and  $\mathbf{k}_2 = (\mathbf{p}_2 - \mathbf{p}'_2)/2$ , respectively. The center-of-mass momentum  $\mathbf{P} = \mathbf{p}_1 + \mathbf{p}'_1 = \mathbf{p}_2 + \mathbf{p}'_2$  is a conserved quantity.

where  $\omega$  is the starting energy of the two interacting electrons in the initial state and  $Q$  is the Pauli operator which excludes all the occupied single-particle levels from the intermediate states of the multiple-scattering processes.

Because it is convenient for many applications to treat the first-order term  $V$  separately, we define the second- and higher-order terms of the  $G$  operator as an effective interaction and refer to as the  $g$  matrix hereafter as shown in Fig. 1. Then the  $g$  matrix in momentum space is described by

$$\begin{aligned} \langle \mathbf{k}_1 \mathbf{P} | g | \mathbf{k}_2 \mathbf{P} \rangle &= \langle \mathbf{k}_1 \mathbf{P} | V \frac{Q}{\omega - H_0} V | \mathbf{k}_2 \mathbf{P} \rangle \\ &+ \langle \mathbf{k}_1 \mathbf{P} | V \frac{Q}{\omega - H_0} g | \mathbf{k}_2 \mathbf{P} \rangle, \end{aligned} \quad (2)$$

where  $\mathbf{P}$  is the center-of-mass momentum of the two interacting particles, and  $\mathbf{k}_1$  and  $\mathbf{k}_2$  are the final and the initial relative momenta as shown in Fig. 1, and  $\omega$  is taken to be  $P^2/4 + k_2^2$  so that the ket vector is on its energy shell.

Note that the  $g$  matrix represents an attractive interaction, which is understood as follows. The multiple-scattering processes induce distortions in the uncorrelated many-body wave function in order to reduce the repulsive potential between electrons. The  $g$  matrix translates this effect into an effective interaction for uncorrelated states, and therefore it is necessarily an attractive interaction.

### B. Partial-wave decomposition

Here we present how to solve Eq. (2) using the partial-wave decomposition for the 2D system<sup>17</sup> to fix the notation. Because the center-of-mass momentum  $\mathbf{P}$  is a conserved quantity, the solution to Eq. (2) may be written as  $\langle \mathbf{k}_1 | g_P | \mathbf{k}_2 \rangle$ . We interpret  $g_P$  as an effective interaction which operates on the relative wave function with the fixed  $\mathbf{P}$ .

Now we perform the partial-wave decomposition of Eq. (2) by using the expansion  $\exp(i\mathbf{k} \cdot \mathbf{r}) = \sum_{n=-\infty}^{\infty} i^n J_n(kr) \exp[in(\theta - \phi)]$  of the 2D plane wave, where  $\mathbf{k} = (k, \theta)$  and  $\mathbf{r} = (r, \phi)$ , and  $J_n$  is the Bessel function. The angles  $\theta$  and  $\phi$  are measured from the fixed direction of  $\mathbf{P}$ .

The Coulomb interaction is given by

$$\delta(\mathbf{r}_1 - \mathbf{r}_2) \exp(-\mu r_1) / r_1$$

in the (relative) coordinate space. Here we have introduced a cutoff parameter  $\mu (> 0)$  which can be chosen to be small enough (typically  $\leq 0.1k_f$ ) not to affect our final results. Then we can express the matrix element of the Coulomb interaction in momentum space as

$$\begin{aligned} \langle \mathbf{k}_1 | V | \mathbf{k}_2 \rangle &= \sum_{n_1, n_2 = -\infty}^{\infty} (-i)^{n_1} \frac{e^{in_1 \theta_1}}{\sqrt{2\pi}} \\ &\times \langle k_1 n_1 | V | k_2 n_2 \rangle i^{n_2} \frac{e^{-in_2 \theta_2}}{\sqrt{2\pi}}, \end{aligned} \quad (3)$$

where the partial-wave components are calculated as

$$\langle k_1 n_1 | V | k_2 n_2 \rangle = \delta_{n_1 n_2} \frac{4\pi}{\sqrt{k_1 k_2}} Q_{|n_1| - 1/2} \left( \frac{k_1^2 + k_2^2 + \mu^2}{2k_1 k_2} \right), \quad (4)$$

with the Legendre function of the second kind  $Q_n$ .

Next, the partial-wave decomposition of the Pauli operator, which has an explicit dependence on the center-of-mass momentum  $\mathbf{P}$ , is given by

$$\begin{aligned} \langle \mathbf{k}_1 | Q_P | \mathbf{k}_2 \rangle &= (2\pi)^2 \delta(\mathbf{k}_1 - \mathbf{k}_2) \theta \left( \left| \frac{\mathbf{P}}{2} + \mathbf{k}_1 \right| - k_f \right) \\ &\times \theta \left( \left| \frac{\mathbf{P}}{2} - \mathbf{k}_1 \right| - k_f \right) \\ &= (2\pi)^2 \frac{\delta(k_1 - k_2)}{k_1} \sum_{n_1, n_2} (-i)^{n_1} \frac{e^{in_1 \theta_1}}{\sqrt{2\pi}} \\ &\times \langle n_1 | Q_P(k_1) | n_2 \rangle i^{n_2} \frac{e^{-in_2 \theta_2}}{\sqrt{2\pi}}, \end{aligned} \quad (5)$$

where

$$\langle n_1 | Q_P(k) | n_2 \rangle = \begin{cases} \delta_{n_1, n_2}, & k_f \leq \left| \frac{P}{2} - k \right| \\ \frac{1 + (-1)^N}{2} \frac{2\gamma \sin N\gamma}{\pi N\gamma}, & \left| \frac{P}{2} - k \right| \leq k_f \leq \sqrt{\frac{P^2}{4} + k^2} \\ 0, & \text{otherwise.} \end{cases} \quad (6)$$

In the above expression, we have defined

$$\gamma = \sin^{-1} \left( \frac{\frac{P^2}{4} + k^2 - k_f^2}{Pk} \right), \quad N = n_1 - n_2, \quad (7)$$

and it is assumed that  $\sin N\gamma / N\gamma = 1$  for  $N = 0$ .

Finally we expand the  $g$ -matrix elements in the same way as Eq. (3) for  $V$ . With all the partial-wave decompositions in the above, Eq. (2) reduces to the following one-dimensional integral equation:

$$\begin{aligned}
\langle k_1 n_1 | g_P | k_2 n_2 \rangle &= \sum_{n, n'} \int_0^\infty \frac{k dk}{(2\pi)^2} \langle k_1 n_1 | V | kn \rangle \\
&\times \frac{\langle n | Q_P(k) | n' \rangle}{k_2^2 - k^2 + i\eta} \langle kn' | V | k_2 n_2 \rangle \\
&+ \sum_{n, n'} \int_0^\infty \frac{k dk}{(2\pi)^2} \langle k_1 n_1 | V | kn \rangle \\
&\times \frac{\langle n | Q_P(k) | n' \rangle}{k_2^2 - k^2 + i\eta} \langle kn' | g_P | k_2 n_2 \rangle, \quad (8)
\end{aligned}$$

which can be solved by the matrix inversion method.<sup>10</sup> Provided that the two particles in the initial states are below the Fermi surface, the energy denominator of Eq. (8) cannot vanish, and therefore the  $g$ -matrix elements are real and satisfy  $\langle k_1 n_1 | g_P | k_2 n_2 \rangle = \langle k_1 - n_1 | g_P | k_2 - n_2 \rangle$ .

In order to remove the dependence on  $\mathbf{P}$  of the  $g$ -matrix elements and to obtain an effective interaction as a function only of the relative coordinates, we fix in Eq. (8) the magnitude of the center-of-mass momentum as  $P = \sqrt{2}k_f$  because of the following reasons. First,  $P = \sqrt{2}k_f$  is the average for all the two-particle states below the Fermi level with vanishing relative momentum, which shall be shown later to be relevant for the derivation of the effective interaction. Second, we have found that the dependence of the matrix element  $\langle \mathbf{k}_1 | g_P | \mathbf{k}_2 \rangle$  on  $P$  is moderate, and also that its average over  $P$  can be approximated well by its value at  $P = \sqrt{2}k_f$ . Next, we take the average over the direction of  $\mathbf{P}$  to make the resultant interaction to be rotationally invariant. After these manipulations, we obtain the following  $g$  matrix, which is rotationally invariant and is a function of  $\mathbf{k}_1$  and  $\mathbf{k}_2$  only:

$$\langle \mathbf{k}_1 | g | \mathbf{k}_2 \rangle = \frac{1}{2\pi} \sum_{n=0}^{\infty} \epsilon_n \langle k_1 n | g | k_2 n \rangle \cos n(\theta_1 - \theta_2), \quad (9)$$

where  $\epsilon_n = 1$  or  $2$  according to  $n=0$  or  $n \neq 0$ .

At the end, we make a remark on the Pauli operator. Note that the exact Pauli operator of Eq. (6)—which we have introduced in the present work—is not rotationally invariant, and therefore couples different angular momenta  $n$ , as can be seen in Eq. (8). In the market, however, the angle-averaged Pauli operator is widely used,<sup>10,13</sup> which is obtained by retaining only the  $n_1 = n_2$  terms in the exact Pauli operator of Eq. (6), and therefore neglects the couplings between different partial waves. The difference between the exact and the angle-averaged Pauli operators is discussed in Ref.<sup>11</sup> for the medium-energy nucleon scatterings off nuclei. They have found that the difference is small, which originates most probably from the short-range nature of the nucleon-nucleon interaction. We shall see, however, that a sizable difference can be produced by these two Pauli operators in the case of the 2DEG.

### C. Separable potential

By taking the Fourier transform of Eq. (9), we may arrive at the effective interaction in the coordinate space  $\langle \mathbf{r}_1 | g | \mathbf{r}_2 \rangle$ .

It is, however, of finite range and nondiagonal with respect to the initial and the final relative coordinates  $\mathbf{r}_2$  and  $\mathbf{r}_1$  (nonlocal interaction), which is not very useful for practical applications. In order to obtain a usable interaction, we propose two new steps. The first step could be referred to as a separable approximation which we now explain and justify. The second step is an expansion around a zero-range potential that will be introduced in the following section.

In our separable approximation, we assume that the  $g$ -matrix elements of Eq. (9) can be approximated by a product of a nonlocal part  $u(p)$  and a local part  $v(q)$  as follows:

$$\langle \mathbf{k}_1 | g | \mathbf{k}_2 \rangle \Rightarrow u(\frac{1}{2}|\mathbf{k}_1 + \mathbf{k}_2|)v(|\mathbf{k}_1 - \mathbf{k}_2|) = u(p)v(q), \quad (10)$$

where we have introduced  $p = |\mathbf{p}| = |\mathbf{k}_1 + \mathbf{k}_2|/2$  and  $q = |\mathbf{q}| = |\mathbf{k}_1 - \mathbf{k}_2|$ . This expression assumes that the  $p$  and  $q$  dependences of the  $g$  matrix is *separable*. Note that the separable approximation in the usual sense assumes the separability with respect to  $\mathbf{k}_1$  and  $\mathbf{k}_2$ .<sup>18</sup> Taking the Fourier transform of Eq. (10), we obtain the separable potential in the coordinate space:

$$\langle \mathbf{r}_1 | g | \mathbf{r}_2 \rangle \Rightarrow \tilde{u}(|\mathbf{r}_1 - \mathbf{r}_2|)\tilde{v}(\frac{1}{2}|\mathbf{r}_1 + \mathbf{r}_2|) = \tilde{u}(s)\tilde{v}(r), \quad (11)$$

where  $s = |s| = |\mathbf{r}_1 - \mathbf{r}_2|$  and  $r = |r| = |\mathbf{r}_1 + \mathbf{r}_2|/2$  are introduced. In case of  $\tilde{u}(|\mathbf{r}_1 - \mathbf{r}_2|) \propto \delta(\mathbf{r}_1 - \mathbf{r}_2)$ , the above interaction reduces to the familiar two-body local interaction which is diagonal with respect to the relative coordinates.

In the separable approximation,  $v(q)$  and  $u(p)$  of Eq. (10) are calculated in the following way. First, we remove the ambiguity in the normalization of  $v(q)$  and  $u(p)$  defined in Eq. (10) by requiring  $u(0) = 1$ . Then by using the forward- and the backward-scattering kinematics in Eqs. (9) and (10), we obtain

$$u(p) = \frac{1}{v(0)} \frac{1}{2\pi} \sum_{n=0}^{\infty} \epsilon_n \langle pn | g | pn \rangle, \quad (12)$$

$$v(q) = \frac{1}{2\pi} \sum_{n=0}^{\infty} \epsilon_n (-1)^n \left\langle \frac{q}{2} n \left| g \right| \frac{q}{2} n \right\rangle. \quad (13)$$

In Fig. 2 we plot how each partial wave contributes in Eqs. (12) and (13) for  $p$  and  $q$  up to several times the Fermi momentum in order to show the global structure of the calculation for  $r_s = 5$ . It can be seen that all the partial-wave contributions show a rapid increase in magnitude around  $p \sim k_f$  for  $u(p)$  and  $q \sim 2k_f$  for  $v(q)$ . This is explained as follows. As  $p$  increases toward  $k_f$ , both of the interacting particles come close to the Fermi level. These particles can be excited from the Fermi sea with a large amplitude because only a small momentum transfer is necessary, which results in the rapid increase of  $\langle pn | g | pn \rangle$  for  $p \sim k_f$ . It is clear that the same argument explains the increase of each partial-wave component around  $q \sim 2k_f$  for  $v(q)$ . The numerical results show also that  $u(p)$  in the range  $p \leq 0.6k_f$  and  $v(q)$  in the range  $q \leq 1.2k_f$  can be reproduced only by the  $s$  and  $p$  waves within an error of 5% for  $r_s \leq 20$ . This derives from the fact that  $\langle kn | g | kn \rangle \propto k^{2n}$  for small  $k$ , as can be easily shown by examining the second-order term of Eq. (8). The above

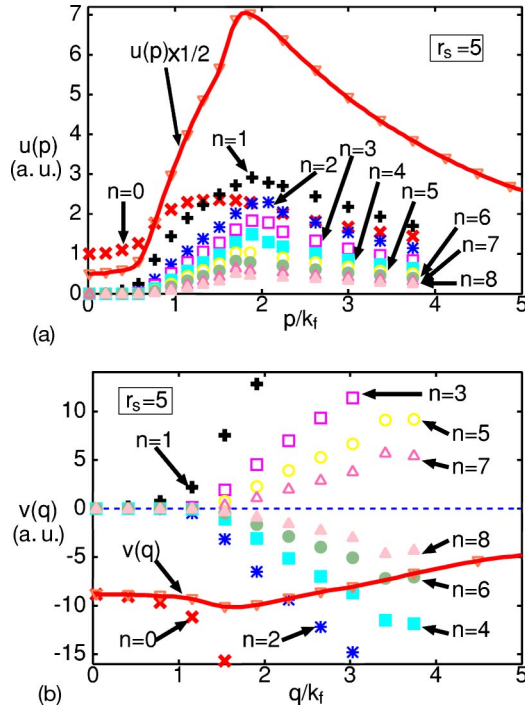


FIG. 2. (Color online) Partial-wave contributions to  $u(p)$  and  $v(q)$  of Eqs. (12) and (13) at  $r_s=5$  in atomic unit.

observation shows that most of the correlations can be described by the  $s$ - and  $p$ -wave processes for the particles below the Fermi level.

From the figure, we can extract the following information on the separable potential  $\tilde{u}(s)\tilde{v}(r)$  in coordinate space. The figure indicates that  $u(p)$  can be expressed as a difference between a slowly decreasing function which dominates the large  $p$  region and a rapidly decreasing function  $\propto \exp(-p^2/k_f^2)$  which controls the small  $p$  behaviors. This observation shows that the nonlocal part  $\tilde{u}(s)$  in coordinate space has a range  $a_u \sim 1/k_f$ . Using a similar argument, we can recognize that  $v(q)$  behaves as  $\propto \exp(-q^2/2k_f^2)$  in the small  $q$  region, and therefore that the local part  $\tilde{v}(r)$  in coordinate space has a range  $a_v \sim 1/2k_f$ . Note that the above argument is valid for any value of  $r_s$ .

Now we are to justify the separable approximation. In order to show how the separable potential  $u(p)v(q)$  fits the original  $g$ -matrix element  $\langle \mathbf{k}_1 | g | \mathbf{k}_2 \rangle$ , we list  $\chi^2$  parameters for the goodness of the separable potential fitting at  $r_s=1, 5, 10$ , and  $20$  in Table I. Comparisons are made for the kinematics with  $k_1=k_2=k \leq k_f/\sqrt{2}$  and  $\theta = \theta_1 - \theta_2 = 0, \pi/4, \pi/2, 3\pi/4$ , and  $\pi$ . This range of  $k$  guarantees that there is no real scattering. From the table, we recognize that the separable potential reproduces the  $g$ -matrix elements with high precision for any kinematics in the range  $r_s \leq 20$ . Especially the  $g$ -matrix elements for  $\theta=0, \pi$  are used to calculate  $u(p)$  and  $v(q)$ , and hence can be reproduced by the separable potential exactly. The range of the validity,  $r_s \leq 20$ , of the separable potential originates from the rapidly increasing error around  $r_s \sim 20$  for the extreme kinematics  $k \sim k_f/\sqrt{2}$ ,  $\theta = \pi/4$ .

TABLE I.  $\chi^2$  parameters for the goodness of the separable potential fitting at  $r_s=1, 5, 10$ , and  $20$  for  $\theta = \theta_1 - \theta_2$  being  $0, \pi/4, \pi/2, 3\pi/4$ , and  $\pi$ .

$\theta$	$r_s=1$	$r_s=5$	$r_s=10$	$r_s=20$
0	0.0	0.0	0.0	0.0
$\pi/4$	0.00227	0.109	0.856	4.30
$\pi/2$	0.0209	0.0190	0.0433	0.414
$3\pi/4$	0.0115	0.0269	0.0256	0.0112
$\pi$	0.0	0.0	0.0	0.0

From all these inspections, we conclude that the  $g$ -matrix element  $\langle \mathbf{k}_1 | g | \mathbf{k}_2 \rangle$  is approximated in an excellent way by the separable potential  $u(p)v(q)$  for the particles below the Fermi surface in the range  $r_s \leq 20$ .

#### D. Skyrme potential

The separable potential  $u(p)v(q)$  in momentum space defines  $\tilde{u}(s)\tilde{v}(r)$  of Eq. (11) in coordinate space. Here we show that  $\tilde{u}(s)\tilde{v}(r)$  assumes a very simple form (momentum-dependent zero-range interaction of Skyrme-type<sup>16</sup>) for the particles below the Fermi level.

The method we adopt here is closely related to the density-matrix expansion<sup>19,20</sup> used in the field of nuclear physics. The most microscopic derivation of the Skyrme interaction from the  $G$  operator is presented in Ref. 20, which treats the medium-energy proton scattering off nuclei. They first expand the nonlocal (one-body) density matrix in the target nucleus to construct an (one-body) optical potential for the projectile proton by folding the nonlocal  $G$  operator of finite range. Then they can define the zero-range effective nucleon-nucleon interaction in such a way that it gives the same optical potential by the folding procedure. Their method obviously assumes the zero rangeness at the final stage, which may be justified in an *ad hoc* manner for the nucleon-nucleon effective potential.

Though their procedure worked out well, we propose a different method, first because we are not treating a high-energy electron which corresponds to the projectile proton of several hundred MeV, and second because we want a direct and fully microscopic definition of the effective interaction without resorting to the one-body (optical) potential.

The matrix element of the  $g$  matrix between arbitrary states  $|\psi\rangle$  and  $|\varphi\rangle$  can be expressed in the separable approximation as

$$\begin{aligned} \langle \psi | g | \varphi \rangle &= \int d\mathbf{r}_1 d\mathbf{r}_2 \psi^* \left( \mathbf{r} + \frac{\mathbf{s}}{2} \right) \tilde{u}(s) \tilde{v}(r) \varphi \left( \mathbf{r} - \frac{\mathbf{s}}{2} \right) \\ &= \int d\mathbf{r} \psi^*(\mathbf{r}) g(\mathbf{r}, \nabla) \varphi(\mathbf{r}). \end{aligned} \quad (14)$$

Here we have translated the separable (nonlocal) potential into the local, but momentum-dependent interaction

$$g(\mathbf{r}, \nabla) = \int ds \exp\left(\frac{s}{2} \cdot \vec{\nabla}\right) \tilde{u}(s) \tilde{v}(r) \exp\left(-\frac{s}{2} \cdot \vec{\nabla}\right), \quad (15)$$

where  $\nabla = \partial/\partial \mathbf{r}$  operates on the relative coordinate.

First, let us note that we can assume in Eq. (15) that the maximum value that  $\nabla$  takes on is of the order of  $k_f$  for particles in the ground and low-lying excited states. Second, we have seen in the preceding section that the range of the nonlocal part  $\tilde{u}(s)$  in coordinate space is given by  $a_u \sim 1/k_f$ . This means that  $|\nabla \cdot s/2| \lesssim 1$  is satisfied in Eq. (15), and therefore we can evaluate Eq. (15) by expanding the exponential. Note that the above procedure is different from the density-matrix expansion<sup>19,20</sup> in that it is an expansion with respect to the nonlocality for the relative coordinate of the initial and the final wave functions. Using a similar argument based on the fact that the range of  $\tilde{v}(r)$  is  $a_v \sim 1/2k_f$ , we can expand  $\tilde{v}(r)$  around a zero-range interaction. By collecting all the terms of the expansion up to second order in  $\nabla$ , we arrive at the following final expression for the effective interaction:

$$g_{skm}(\mathbf{r}, \nabla) = \alpha \delta(\mathbf{r}) + \beta \{\vec{\nabla}^2 \delta(\mathbf{r}) + \delta(\mathbf{r}) \vec{\nabla}^2\} + 2\gamma \vec{\nabla} \delta(\mathbf{r}) \cdot \vec{\nabla}. \quad (16)$$

Here the coefficients  $\alpha$ ,  $\beta$ , and  $\gamma$  are given by

$$\alpha = v_0, \quad \beta = \frac{1}{16} v_0 u_2 + \frac{1}{4} v_2, \quad \gamma = -\frac{1}{16} v_0 u_2 + \frac{1}{4} v_2, \quad (17)$$

in terms of the moments  $u_i$  and  $v_j$  of  $\tilde{u}(s)$  and  $\tilde{v}(r)$  defined by

$$u_i = 2\pi \int_0^\infty s ds s^i \tilde{u}(s), \quad i=0,2,\dots, \quad (18)$$

$$v_j = 2\pi \int_0^\infty r dr r^j \tilde{v}(r), \quad j=0,2,\dots \quad (19)$$

The effective interaction of Eq. (16) is a zero-range momentum-dependent Skyrme-type interaction which has been extensively used in nuclear physics.<sup>16,19</sup> The moments  $u_i$  and  $v_i$  can be calculated numerically from the potential in momentum space as

$$u_0 = u(0) = 1, \quad v_0 = v(0),$$

$$u_2 = -2 \frac{d^2}{dp^2} u(p) \Big|_{p=0}, \quad v_2 = -2 \frac{d^2}{dq^2} v(q) \Big|_{q=0}.$$

The above expressions, together with Eqs. (12) and (13), show that we need only the diagonal  $g$ -matrix elements  $\langle kn|g|kn \rangle$  in the low-energy limit ( $k \sim 0$ ) to obtain the effective interaction  $g_{skm}(\mathbf{r}, \nabla)$  of Eq. (16). Let us recall that  $\langle kn|g|kn \rangle \propto k^{2n}$  for small  $k$ , which shows that only the  $n=0,1$  terms contribute to the above coefficients. This is a direct consequence of the fact that the first two terms on the right-hand side (rhs) of Eq. (16) represent the  $s$ -wave ( $n=0$ ) interaction and the third the  $p$ -wave ( $n=1$ ) interaction.

TABLE II. Interaction strengths  $\alpha$ ,  $\beta$ , and  $\gamma$  in atomic unit of the effective interaction  $g_{skm}(\mathbf{r}, \nabla)$  of Eq. (16).

$r_s$	$\alpha$	$\beta$	$\gamma$
0.1	$-0.10362 \times 10^{-1}$	$0.19810 \times 10^{-4}$	$-0.68883 \times 10^{-5}$
0.3	$-0.89084 \times 10^{-1}$	$0.14245 \times 10^{-2}$	$-0.54085 \times 10^{-3}$
0.5	$-0.23040 \times 10^{+0}$	$0.98441 \times 10^{-2}$	$-0.40356 \times 10^{-2}$
1	$-0.78034 \times 10^{+0}$	$0.12478 \times 10^{+0}$	$-0.59877 \times 10^{-1}$
3	$-0.43625 \times 10^{+1}$	$0.54584 \times 10^{+1}$	$-0.37789 \times 10^{+1}$
5	$-0.88408 \times 10^{+1}$	$0.28806 \times 10^{+2}$	$-0.24058 \times 10^{+2}$
10	$-0.21315 \times 10^{+2}$	$0.25990 \times 10^{+3}$	$-0.27247 \times 10^{+3}$
15	$-0.34535 \times 10^{+2}$	$0.92342 \times 10^{+3}$	$-0.10794 \times 10^{+4}$
20	$-0.48114 \times 10^{+2}$	$0.22588 \times 10^{+4}$	$-0.28187 \times 10^{+4}$

The matrix element of  $g_{skm}(\mathbf{r}, \nabla)$  in momentum space is given by

$$\langle \mathbf{k}_1 | g_{skm} | \mathbf{k}_2 \rangle = \alpha - \beta(k_1^2 + k_2^2) + 2\gamma \mathbf{k}_1 \cdot \mathbf{k}_2. \quad (20)$$

Let us compare Eq. (20) with the original  $g$ -matrix elements  $\langle \mathbf{k}_1 | g | \mathbf{k}_2 \rangle$  for  $r_s \leq 20$ , using the same kinematics as for the separable potential. We have found that the simple effective interaction  $g_{skm}(\mathbf{r}, \nabla)$  represents the original  $g$ -matrix elements  $\langle \mathbf{k}_1 | g | \mathbf{k}_2 \rangle$  as a whole at a satisfactory level. This is understandable because the separable potential  $u(p)v(q)$  in the relevant range can be reproduced mostly by the  $s$  and  $p$  waves only.

To summarize, we have presented a fully microscopic derivation of the effective interaction operator  $g_{skm}(\mathbf{r}, \nabla)$ , which is expressed in terms of the three parameters only ( $\alpha$ ,  $\beta$ , and  $\gamma$ ), and represents the multiple-scattering processes in the medium very well in the range  $r_s \leq 20$ .

### III. RESULTS AND DISCUSSION

#### A. Skyrme potential

The Skyrme-type interaction  $g_{skm}(\mathbf{r}, \nabla)$  of Eq. (16) characterizes the short-range correlation in terms of the  $s$ - and  $p$ -wave scattering processes, and is convenient also to study the momentum dependence of the correlation.

We present the numerical results for the coefficients  $\alpha$ ,  $\beta$ , and  $\gamma$  in Table II for several values of  $r_s$ , and also in Fig. 3 in the range  $0 \leq r_s \leq 10$ . Let us examine the  $r_s$  dependences of  $\alpha$ ,  $\beta$ , and  $\gamma$ . As shown in Fig. 3, numerical results show that they can be reproduced qualitatively by

$$\alpha \sim \alpha(r_s=1) \times r_s^{1.5} \sim -0.8 r_s^{1.5},$$

$$\beta \sim \beta(r_s=1) \times r_s^{3.4} \sim +0.1 r_s^{3.4}, \quad (21)$$

$$\gamma \sim \gamma(r_s=1) \times r_s^{3.7} \sim -0.06 r_s^{3.7}.$$

In order to explain the above  $r_s$  dependences, we examine the  $g$ -matrix elements  $\langle kn|g|kn \rangle$  for  $n=0$  and 1 for small values of  $k$ , which is given by the following expansion using  $\alpha$ ,  $\beta$ , and  $\gamma$ :

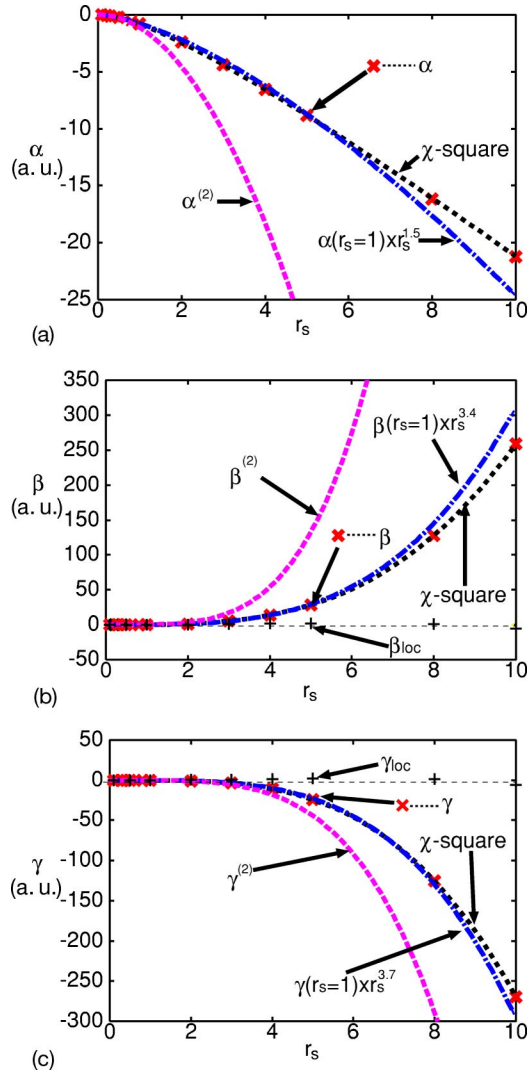


FIG. 3. (Color online) Coefficients  $\alpha$ ,  $\beta$  and  $\gamma$  of the effective interaction  $g_{skm}(\mathbf{r}, \nabla)$  in atomic unit. The dotted lines denoted by  $\chi$  square stand for the formulas (24), (25) and (26). The dotted-dashed lines represent the simple formulas in Eq. (21).  $\alpha^{(2)}$ ,  $\beta^{(2)}$ , and  $\gamma^{(2)}$  represent the second-order results of Eq. (23). Solid crosses  $\beta_{loc}$  and  $\gamma_{loc}$  represent the calculation without the nonlocal effect, obtained by setting  $u_2=0$ .

$$\frac{1}{2\pi} \langle kn | g | kn \rangle = \begin{cases} \alpha - 2\beta k^2, & n=0 \\ \gamma k^2, & n=1. \end{cases} \quad (22)$$

By looking into the second-order (leading) term of Eq. (8) for small values of  $k$ , and by comparing it with the above expression, we obtain

$$\alpha^{(2)} \sim -r_s^2, \quad \beta^{(2)} \sim 0.2 r_s^4, \quad \gamma^{(2)} \sim -0.07 r_s^4, \quad (23)$$

where  $\alpha^{(2)}$ ,  $\beta^{(2)}$ , and  $\gamma^{(2)}$  are the second-order results for  $\alpha$ ,  $\beta$ , and  $\gamma$ , respectively. In Fig. 3 we can see that the second-order terms reproduce qualitative behaviors of  $\alpha$ ,  $\beta$ , and  $\gamma$  especially in the small  $r_s$  region. Because an iterative solution to Eq. (8) makes an alternate series because of the

TABLE III. Parameters of the fitting formulas (24), (25), and (26) for the strengths  $\alpha$ ,  $\beta$ , and  $\gamma$  in atomic unit.

$a_1$	-1.1533	$b_1$	0.24796	$c_1$	-0.071295
$a_2$	0.25643	$b_2$	0.076771	$c_2$	0.21673
$a_3$	0.50131	$b_3$	0.93833	$c_3$	0.20596
$a_4$	0.094028	$b_4$	0.038957	$c_4$	0.021031

negative-energy denominator, the convergent results for  $\alpha$ ,  $\beta$ , and  $\gamma$  of Eq. (21) show slightly weaker  $r_s$  dependences than those in Eq. (23).

We recognize that  $\beta$  and  $\gamma$  grow much more rapidly than  $\alpha$  with decreasing density. Note that the  $\beta$  and  $\gamma$  terms in  $g_{skm}(\mathbf{r}, \nabla)$  are momentum dependent, and express the interaction which put emphasis on high-momentum components of the relative wave function. Then it is naturally understood that the increasing importance of the short-range correlation with decreasing density manifests itself in the rapidly growing strengths  $\beta$  and  $\gamma$ .

If we look into  $\beta$  and  $\gamma$  more closely, we recognize that they satisfy  $\beta \sim -3\gamma$  in the small  $r_s$  region as indicated by the second-order results, and also that  $\gamma \propto r_s^{3.7}$  increases faster than  $\beta \propto r_s^{3.4}$  in the large  $r_s$  regime, showing explicitly the growing importance of the  $p$ -wave contribution with increasing  $r_s$ .

In order to show the strong nonlocal aspect of the effective interaction, we have presented  $\beta_{loc}$  and  $\gamma_{loc}$  that are calculated without the nonlocality by setting  $u(p)=1$  ( $u_2=0 \Rightarrow \beta_{loc} = \gamma_{loc} = \frac{1}{4}v_2$ ) in Fig. 3. We can see clearly from the figure that the momentum-dependent terms  $\beta$  and  $\gamma$  of the effective interaction represent mostly the effect of the nonlocality of the  $g$  matrix.

Finally, we fit  $\alpha$ ,  $\beta$ , and  $\gamma$  by the  $\chi$ -square method in the following form:

$$\alpha = a_1 x^4 \frac{1 + a_2 x}{1 + a_2 x + a_3 x^2 + a_4 x^3}, \quad (24)$$

$$\beta = b_1 x^8 \frac{1 + b_2 x}{1 + b_2 x + b_3 x^2 + b_4 x^3}, \quad (25)$$

$$\gamma = c_1 x^8 \frac{1 + c_2 x}{1 + c_2 x + c_3 x^2 + c_4 x^3}, \quad (26)$$

where  $x = \sqrt{r_s}$ . All the coefficients in the above expressions are given in Table III. They are obtained using 15 data points for  $r_s$ , ranging from 0.1 to 20. The above formulas reproduce the original data very well, as shown by their  $\chi^2$  parameters  $1.23 \times 10^{-4}$ ,  $7.09 \times 10^{-4}$ , and  $3.92 \times 10^{-6}$  for  $\alpha$ ,  $\beta$ , and  $\gamma$ , respectively.

The above expressions assume that the  $g$  matrix vanishes as  $r_s \rightarrow 0$ , because the Pauli operator in the rhs of Eq. (2) suppresses all the multiple-scattering processes in the high-density limit. We also notice that the effective interaction becomes significantly larger in the low-density limit. This is understandable because the  $g$  matrix in this limit describes

the Coulomb scattering in free space which gives a divergent  $T$  matrix in the low-energy limit.<sup>17</sup>

At the end of this subsection, let us think of an implication of the above interaction in real 2D systems such as quantum dots. It is straightforward to show the expression,  $1/m^* = 1 - \rho(\beta - 3\gamma)/2 + \text{exchange contribution}$ , for the effective mass  $m^*$  in the Brueckner-Hartree-Fock (BHF) calculation in the same way as for 3D systems.<sup>21</sup> The HF theory takes into account only the exchange contribution that reduces the effective mass, which in turn makes large energy spacings around the Fermi level. On the other hand, in the BHF calculation, the short-range correlation realized by the  $g$  matrix tends to cancel the exchange contribution to reduce the energy spacings of the HF theory, as is clear from the above expression. This implies, for example, that the system is softer in the BHF theory than in the HF theory, as is the case for 3D clusters.<sup>14</sup> We expect, therefore, that the polarizability, for example, would be an appropriate observable to discuss the effects of the  $g$  matrix.

### B. Separable potential

Here we examine the properties of the separable potential  $\tilde{u}(s)\tilde{v}(r)$  in the coordinate space, which features the local and nonlocal aspects of the short-range correlation. As stated before, numerical results show that  $u(p)v(q)$  can be mostly reproduced only by the  $s$  and  $p$  waves for the particles below the Fermi level. This allows us to discuss the separable potential in terms of the  $s$ - and  $p$ -wave contributions.

Let us start with the second moment  $v_2 = 2(\beta + \gamma)$  of the local part  $\tilde{v}(r)$ , which comes out of the cancellation between the  $s$  and  $p$  waves. While  $r_s$  is small, the lowest-order results,  $\beta \sim -3\gamma$ , of Eq. (23) holds, and therefore  $v_2$  is positive. As  $r_s$  increases, the  $p$ -wave term  $\gamma$  grows faster than the  $s$ -wave term  $\beta$ , ultimately to make  $v_2$  negative around  $r_s \sim 8.5$ , and then  $v_2$  decreases rapidly. Let us recall that the second moment  $v_2$  puts more stress on the long-range part of  $\tilde{v}(r)$  than the zeroth moment  $v_0$  which is negative. Then the above  $r_s$  dependence of  $v_2$  means that  $\tilde{v}(r)$  is attractive at short distances, but behaves as a repulsive potential for large separations in the small  $r_s$  region.

Next, we come to the second moment  $u_2$  of the nonlocal part  $\tilde{u}(s)$ . We can easily realize that the magnitude of  $u_2 = 8(\beta - \gamma)/v_0$  is a strongly increasing function of  $r_s$ , because  $\beta$  and  $\gamma$  contribute coherently, in contrast with the case of  $v_2$ . This means that the nonlocal aspect featured by  $u_2$  of the short-range correlations grows much faster with increasing  $r_s$  than the local counterpart characterized by  $v_2$ .

Let us look into the momentum dependence of  $g_{skm}(\mathbf{r}, \nabla)$ . For  $r_s \geq 10$ , the  $p$ -wave term  $\gamma$  dominates over the  $s$ -wave term  $\beta$ . Then we obtain  $v_2 \cong 2\gamma$  and  $u_2 v_0 \cong -8\gamma$ , and can drop the  $\beta$  term in  $g_{skm}(\mathbf{r}, \nabla)$  of Eq. (16). In this case, the momentum dependence of  $g_{skm}(\mathbf{r}, \nabla)$  originates solely from the nonlocal part  $\tilde{u}(s)$  of the separable potential, and stands only for the  $p$ -wave scattering processes in the medium.

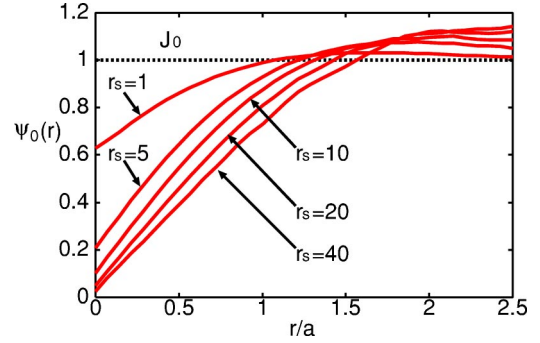


FIG. 4. (Color online) The Bethe-Goldstone wave function  $\psi_0(r)$  for an  $s$ -wave pair with  $P = \sqrt{2}k_f$  (center-of-mass momentum) and  $k=0$  (relative momentum in the asymptotic region) for several values of  $r_s$ . The crossover point of  $\psi_0(r)$  with the free wave function  $J_0(0)=1$  (note  $kr=0$ ) defines the healing distance  $h$ .

### C. Healing property

The  $g$  matrix treats only the two-body correlation, and the three- or many-body dynamical correlations are not taken into account. Here we examine the importance of the three-body correlation by investigating the wave function in the medium.

It is well known that the two-body wave function  $\psi$  for the relative motion in the medium can be obtained from Eq. (1) as

$$\psi = \phi + \frac{Q}{\omega - H_0} V \psi, \quad (27)$$

where the first term  $\phi$  stands for the uncorrelated plane wave and the second term represents the distortion in  $\psi$  which is localized around the origin in the relative coordinate space due to the Pauli operator. This means that the relative wave function  $\psi$  approaches the uncorrelated plane wave  $\phi$  for large separations, which is known as the *healing* property of the two-body wave function in the medium.<sup>22,23</sup>

It is straightforward to decompose the above equation into partial waves as in Sec. II to obtain the  $n$ th partial-wave component  $\psi_n(r)$ . It is conventional to define the healing distance  $h$  (for the  $s$  wave) as the first crossover point of  $\psi_0(r)$  and the free wave, which is shown in Fig. 4 for several values of  $r_s$ . Then the ratio  $(h/d)^2$  measures the size of the *wound* of the wave function  $\psi_0(r)$  in 2D systems, where  $d = 2a$  ( $1/\rho = \pi a^2$ ) is the average interparticle distance.

Because the three-body correlation becomes important when three particles come to the area of the wound simultaneously, it gives a correction of the order of  $(h/d)^4$  to the two-body correlation,<sup>22,23</sup> which is given in Table IV. In (3D) nuclear systems, the corresponding ratio is estimated to be  $(h/d)^6 \sim 0.15$ , which is believed to justify the Brueckner theory as a good starting point to describe nuclear systems.<sup>22,23</sup> From Table IV, we notice that  $(h/d)^4 \sim 0.08$  for  $r_s = 1$ , and therefore that the two-body correlation is dominant. As the density decreases, the wound of the wave function becomes larger, and the ratio  $(h/d)^4$  shows a rapid increase with decreasing density for  $r_s \geq 20$ , giving  $(h/d)^4$

TABLE IV. Healing properties for several values of  $r_s$  shown in Fig. 4. The ratio  $(h/d)^4$  is a measure of the three-body correlation compared with the two-body correlation, where  $d=2a$  is the average interparticle distance.

$r_s$	$h/d$	$(h/d)^4$
1	0.53	0.08
5	0.61	0.14
10	0.65	0.18
20	0.71	0.26
40	0.78	0.38

$\sim 0.26$  at  $r_s=20$  and  $(h/d)^4 \sim 0.38$  at  $r_s=40$ . We then realize that the two-body correlation alone is not in control of the system any more for  $r_s \geq 20$ , and the many-body correlation becomes important. From the standpoint of the  $g$ -matrix theory, such many-body correlations are to be incorporated explicitly in the wave function of a many-body system interacting via the  $g$  matrix.

From the above observation, we conclude that the two-body correlation loses its dominance around  $r_s \sim 20$ , where the separable potential was found to cease to be an excellent approximation in Sec. II.

#### D. Pair-correlation function

In order to clarify the physics represented by the  $g$ -matrix theory from another point of view, we calculate the pair-correlation function  $g(r)$  from the Bethe-Goldstone equation.<sup>13</sup> In Fig. 5, we plot  $g(r)$  of the  $g$ -matrix theory together with the RPA and the quantum Monte Carlo (QMC) calculations for  $r_s=1, 5$ , and 10. We immediately realize that  $g(r)$  of the  $g$ -matrix theory approaches the QMC values in the limit  $r \rightarrow 0$ , while the RPA fails. This shows explicitly the importance of the ladder processes at short distances.

The difference between the  $g$ -matrix theory and the QMC should be attributed to the correlations beyond the ladder processes, which could be expressed, in principle, by three- or many-body interactions. Let us look into the case of  $r_s=1$ . The figure shows that the ladder processes reproduce the QMC results very well for  $r_s=1$  in the whole range of  $r$ . In the case of  $r_s=5$ , the figure indicates that the ladder processes could be supplemented by the RPA-type processes in the range  $r \geq a$ . The figure for  $r_s=10$  shows that the correlations beyond the ladder processes are not under the control of the RPA any more, and also that the difference between the  $g$ -matrix theory and the QMC becomes sizable as the density decreases especially for  $r \geq a$ . This means that the many-body correlations beyond the ladder (and the RPA) processes become important for  $r \geq a$  in the large  $r_s$  regime.

Let us consider how to describe low-lying excited states of the 2DEG using the effective interaction derived from the  $g$  matrix. The problem is how to treat the dynamical correlations beyond the ladder processes incorporated by the  $g$  matrix. The above observation suggests that a hybrid model<sup>13</sup> might work well in the small  $r_s$  region, which interpolates the  $g$ -matrix theory for small separations and the RPA for

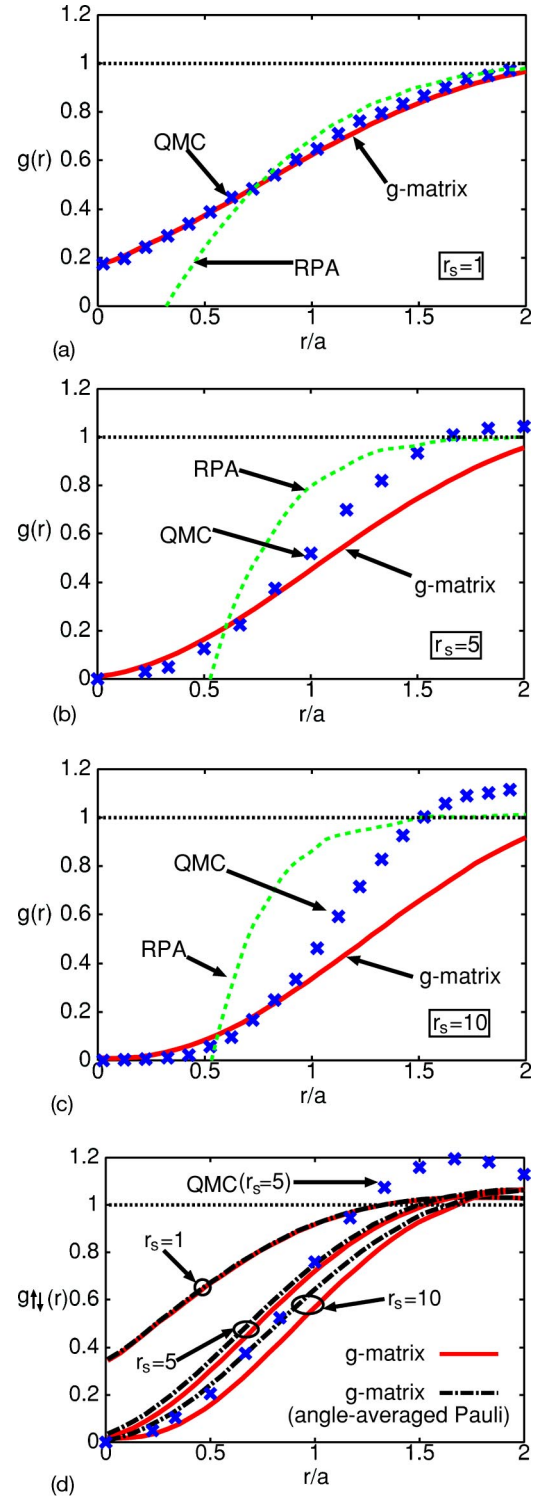


FIG. 5. (Color online) Pair-correlation functions  $g(r)$  and  $g_{\uparrow\downarrow}(r)$  for  $r_s=1, 5$ , and 10. The unit of length is  $a$  which is defined by the density  $\rho$  as  $1/\rho = \pi a^2$ . The QMC results for  $r_s=1, 10$  and  $r_s=5$  are taken from Refs. 26 and 27, respectively. Note that the RPA gives negative values in the small  $r$  region.

large separations. In the large  $r_s$  region, on the other hand, it is strongly indicated that we need to go beyond the RPA description of the state vector, which may be the second RPA (Ref. 24) or the extended RPA.<sup>25</sup>

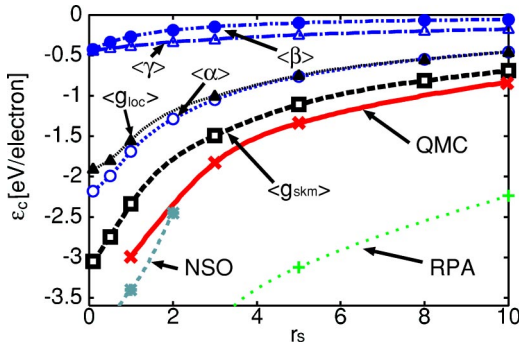


FIG. 6. (Color online) Correlation energy (eV/electron) of the 2DEG. NSO represents the results of Ref. 7.  $\langle g_{skm} \rangle$  represents the correlation energies of Eq. (28) with the exact Pauli operator.  $\langle \alpha \rangle$ ,  $\langle \beta \rangle$ , and  $\langle \gamma \rangle$  represent the contributions of the corresponding terms of the Skyrme interaction of Eq. (16).  $\langle g_{loc} \rangle$  represents the results obtained by dropping the nonlocal effect in Eq. (28).

Finally we compare the exact and the angle-averaged Pauli operators using  $g_{\uparrow\downarrow}(r)$  in Fig. 5, which is free from the Pauli principle and represents the pure dynamical correlation between electrons. The numerical results for  $r_s=5$  shows that  $g_{\uparrow\downarrow}(r)$  with the exact Pauli operator is slightly closer to the QMC than that with the angle-averaged Pauli operator. We can see also that the difference is visible in the range  $r \lesssim a$  and increases with decreasing density. This indicates the importance of the couplings of different angular momenta described by the exact Pauli operator especially for small separations in the low-density region.

### E. Correlation energy

The correlation energy per electron in the ladder approximation can be expressed as

$$\varepsilon_c = \frac{1}{\rho} \langle 0 | g_{skm} | 0 \rangle = \rho \left( \frac{\alpha}{4} - \frac{\beta}{8} k_f^2 + \frac{3\gamma}{8} k_f^2 \right), \quad (28)$$

in terms of the effective interaction of Eq. (16) in the  $g$ -matrix theory,<sup>9</sup> where  $|0\rangle$  stands for the ground state of a noninteracting system.

The correlation energy of Eq. (28) is shown in Fig. 6 and in Table V as  $\langle g_{skm} \rangle$ , together with the RPA and the QMC results.<sup>26,27</sup> We can see that Eq. (28) underestimates the correlation energy of the QMC by about 20%, which is the same order of the magnitude as the estimated contribution of the

TABLE V. Correlation energies of the 2DEG in different theories in unit of eV/electron.  $\langle g_{skm} \rangle$  expresses the correlation energies of Eq. (28), while  $\langle g_{skm} \rangle_{aa}$  represents the results with the angle-averaged Pauli operator.

$r_s$	$\langle g_{skm} \rangle$	$\langle g_{skm} \rangle_{aa}$	QMC	RPA
1	-2.35	-2.43	-2.99	-5.39
3	-1.50	-1.63	-1.83	-3.83
5	-1.11	-1.26	-1.33	-3.12
10	-0.694	-0.834	-0.82	-2.24
20	-0.405	-0.524	-0.47	-1.61

three-body correlation,  $(h/d)^4$ , in Table IV. The discrepancy between the QMC and Eq. (28) could be removed, in principle, if we can include an effective interaction in Eq. (28) whose origin is the many-body correlation, as discussed in the preceding section. It is, however, beyond the scope of the present work.

In the table we have also presented the results for Eq. (28) with the angle-averaged Pauli operator as  $\langle g_{skm} \rangle_{aa}$ . We can realize that the difference between the exact and the angle-averaged Pauli operators becomes sizable with decreasing density. The fact that  $\langle g_{skm} \rangle_{aa}$  is closer to the QMC than  $\langle g_{skm} \rangle$  does not mean that the angle-averaged Pauli operator is better than the exact one, as can be seen in the pair-correlation function.

In Fig. 6, we plot also the three terms on the rhs of Eq. (28) separately as  $\langle \alpha \rangle$ ,  $\langle \beta \rangle$ , and  $\langle \gamma \rangle$ . The line denoted by  $\langle g_{loc} \rangle$  stands for the results obtained by dropping the nonlocality effect by replacing  $\beta \Rightarrow \beta_{loc}$  and  $\gamma \Rightarrow \gamma_{loc}$  in Eq. (28) (see Fig. 3). From the figure we recognize (i) that the  $\alpha$  term is most important in the correlation energy and (ii) that the relative importance of the  $p$ -wave contribution ( $\gamma$  term) becomes appreciable as the density decreases. Because the  $\beta$  and  $\gamma$  terms stem mostly from the nonlocality of the  $g$  matrix ( $\langle g_{loc} \rangle \approx \langle \alpha \rangle$  in this  $r_s$  region), it is clear that the nonlocal feature of the short-range correlation plays an important role in the calculation of the correlation energy. The line denoted by NSO represents the ladder results of Nagano, Singwi, and Ohnishi.<sup>7</sup> It is, however, difficult to compare our results with theirs. First, this is because they assume about 10% error in the results and second because we have expressed the ladder processes as an effective interaction as our first step before calculating  $\varepsilon_c$ .

### IV. SUMMARY

First, we presented in detail a fully microscopic derivation of an effective electron-electron interaction which represents the short-range correlations in the 2DEG. We started from the Bethe-Goldstone equation for the  $g$  matrix which stands for the multiple-scattering processes in the medium. The  $g$  matrix is presented first by the separable potential  $\tilde{u}(s)\tilde{v}(r)$ , and second it is translated into the momentum-dependent zero-range effective interaction  $g_{skm}(\mathbf{r}, \nabla)$  of the Skyrme-type with three parameters only. The Skyrme interaction  $g_{skm}(\mathbf{r}, \nabla)$  has been shown to be valid for the particles below the Fermi surface for  $r_s \lesssim 20$ , and is presented as an explicit function of  $r_s$ .

Second, we examined the short-range correlation in detail using the obtained effective interaction. We have shown that the short-range correlation is highly nonlocal, which originates from both  $s$ - and  $p$ -wave processes for  $r_s \lesssim 10$ , and solely from the  $p$  wave for  $r_s \gtrsim 10$ .

Third, we compared the pair-correlation function and the correlation energy in the  $g$ -matrix theory with those of the QMC calculation to show the physics realized as the effective interaction operator. The importance of the many-body correlations beyond the ladder processes in the low-density region is stressed explicitly, which is responsible for the difference between the  $g$ -matrix theory and the QMC. If one

uses the  $g$  matrix as an effective interaction in the description of a many-body system, one has to incorporate such many-body correlations in the wave function of the system. We have also compared the newly introduced exact Pauli operator with the widely used angle-averaged Pauli operator using these physical quantities. We have shown explicitly that the difference becomes sizable in the low-density region, in contrast with the nuclear systems.

Let us stress that the effective interaction represents the correlations in a very simple fashion, and at the same time it is a very useful tool which can be applied to the description of both the ground and the low-lying excited states. In three-dimensional systems, a similar effective interaction has been applied successfully to the metal cluster in the framework of the Brueckner-Hartree-Fock theory.<sup>14</sup> We believe that our

microscopic effective interaction will be useful in the same way in examining various two-dimensional electron systems such as quantum dots.

Finally we make a comment on experimentally realizable systems, which are different from the pure 2DEG, in that they cannot be free from defects and have some finite width. The effects of the finite width is well under control using form factors.<sup>28</sup> On the other hand, the 2D systems with defects comprise a large field of current research.<sup>29</sup> The incorporation of these two effects in the effective interaction is an open problem for the future.

#### ACKNOWLEDGMENT

We thank Francesco Pederiva for reading the manuscript.

- 
- <sup>1</sup>M.A. Kastner, Rev. Mod. Phys. **64**, 849 (1992); Phys. Today **46** (1), 24 (1993); J.P. Eisenstein, L.N. Pfeiffer and K.W. West, Phys. Rev. Lett. **68**, 674 (1992); M.A. Eriksson, A. Pinczuk, B.S. Dennis, S.H. Simon, L.N. Pfeiffer and K.W. West, *ibid.* **82**, 2163 (1999).
- <sup>2</sup>F. Stern, Phys. Rev. Lett. **18**, 546 (1967).
- <sup>3</sup>D.E. Beck and P. Kumar, Phys. Rev. B **13**, 2859 (1976).
- <sup>4</sup>M. Jonson, J. Phys. C **9**, 3055 (1976); N. Iwamoto, Phys. Rev. B **43**, 2174 (1991); K. Sato and S. Ichimaru, J. Phys. Soc. Jpn. **58**, 787 (1989); A. Gold and L. Calmels, Phys. Rev. B **48**, 11 622 (1993).
- <sup>5</sup>D.L. Freeman, Solid State Commun. **26**, 289 (1978).
- <sup>6</sup>D. Neilson, L. Swierkowski, A. Sjolander, and J. Szymański, Phys. Rev. B **44**, 6291 (1991).
- <sup>7</sup>S. Nagano, K.S. Singwi and S. Ohnishi, Phys. Rev. B **29**, 1209 (1984).
- <sup>8</sup>D.J.W. Geldart and D. Neilson, Phys. Rev. B **67**, 045310 (2003).
- <sup>9</sup>H.A. Bethe and J. Goldstone, Proc. R. Soc. London, Ser. A **238**, 551 (1957); K. Brueckner, R.J. Eden, and N.C. Francis, Phys. Rev. **100**, 891 (1955); J. Hüfner and C. Mahaux, Ann. Phys. (N.Y.) **73**, 525 (1972).
- <sup>10</sup>M.I. Haftel and F. Tabakin, Nucl. Phys. A **158**, 1 (1970).
- <sup>11</sup>T. Cheon and E.F. Redish, Phys. Rev. C **39**, 331 (1989).
- <sup>12</sup>G. Bertsch, J. Borysowicz, and H. McManus, Nucl. Phys. A **284**, 399 (1977); K. Nakayama and W.G. Love, Phys. Rev. C **38**, 51 (1988); T. Cheon and K. Takayanagi, Phys. Rev. Lett. **68**, 1291 (1992); K. Takayanagi and E. Lipparini, Phys. Rev. B **54**, 8122 (1996); D.E. Lansky and Y. Yamamoto, Phys. Rev. C **55**, 2330 (1997); M.K. Banerjee and J.A. Tjon, Nucl. Phys. A **708**, 303 (2002).
- <sup>13</sup>D.N. Lowy and G.E. Brown, Phys. Rev. B **12**, 2138 (1975); K. Bedell and G.E. Brown, *ibid.* **17**, 4512 (1978).
- <sup>14</sup>E. Lipparini, Ll. Serra, and K. Takayanagi, Phys. Rev. B **49**, 16 733 (1994).
- <sup>15</sup>H.V. von Geramb, *The Interactions Between Medium Energy Nucleons in Nuclei—1982*, edited by H. O. Meyer, AIP Conf. Proc. No. 97 (AIP, New York, 1982).
- <sup>16</sup>T.H.R. Skyrme, Philos. Mag. **1**, 1043 (1956); Nucl. Phys. **9**, 615 (1959); M. Beiner, H. Flocard, and N. Van Giai, Nucl. Phys. A **238**, 29 (1975); O. Bohigas, N. Van Giai, and D. Vautherin, Phys. Lett. **102B**, 105 (1981); N. Van Giai and H. Sagawa, Nucl. Phys. A **371**, 1 (1981).
- <sup>17</sup>M. Schick, Phys. Rev. A **3**, 1067 (1971); P. Bloom, Phys. Rev. B **12**, 125 (1975).
- <sup>18</sup>D.J. Ernst, C.M. Shakin, and R.M. Thaler, Phys. Rev. C **8**, 46 (1973); J. Haidenbauer and W. Plessas, *ibid.* **30**, 1822 (1984); N.H. Kwong and H.S. Köhler, *ibid.* **55**, 1650 (1997).
- <sup>19</sup>D. Vautherin and D.M. Brink, Phys. Rev. C **5**, 626 (1972); J.W. Negele and D. Vautherin, *ibid.* **5**, 1472 (1972).
- <sup>20</sup>T. Cheon, Phys. Rev. C **34**, 1173 (1986); **35**, 2225 (1987); **37**, 1088 (1988).
- <sup>21</sup>E. Lipparini and S. Stringari, Phys. Rep. **175**, 103 (1989).
- <sup>22</sup>L.S. Gomes, J.D. Walecka, and V.F. Weisskopf, Ann. Phys. (N.Y.) **3**, 241 (1958); B.D. Day, Rev. Mod. Phys. **39**, 719 (1967).
- <sup>23</sup>A. deShalit and H. Feshbach, *Theoretical Nuclear Physics* (Wiley, New York, 1974), Vol. I; A.L. Fetter and J.D. Walecka, *Quantum Theory of Many-Particle Systems* (McGraw-Hill, New York, 1971).
- <sup>24</sup>C. Yannouleas, M. Dworzecka, and J.J. Griffin, Nucl. Phys. A **397**, 239 (1988).
- <sup>25</sup>K. Takayanagi, K. Shimizu, and A. Arima, Nucl. Phys. A **477**, 205 (1988); **481**, 313 (1988).
- <sup>26</sup>B. Tanatar and D.M. Ceperley, Phys. Rev. B **39**, 5005 (1989).
- <sup>27</sup>F. Rapisarda and G. Senatore, Aust. J. Phys. **49**, 161 (1996).
- <sup>28</sup>A. Gold, Phys. Rev. B **35**, 723 (1987); L. Calmels and A. Gold, *ibid.* **57**, 1436 (1998).
- <sup>29</sup>E. Abrahams, S.V. Kravchenko, and M.P. Sarachik, Rev. Mod. Phys. **73**, 251 (2001).